Texture Formation in Multiphase Polymer-Liquid Crystal Materials

Susanta K. Das and Alejandro D. Rey***

Department of Chemical Engineering, McGill University
3610 University Street, Montreal, Quebec H3A 2B2, Canada.
**susanta.das@staff.mcgill.ca*
***alejandro.rey@mcgill.ca*

Abstract

Texture formation in a binary mixture of a flexible polymer and a liquid crystal has been studied using a nonlocal kinetic model for phase separation in the presence of liquid crystalline order. The model takes into account couplings between phase separation, phase ordering, and texture formation. The phase separation-phase ordering coupling leads to orientation normal to local concentration gradients, while curvature in the isotropic phase leads to defect nucleation in the nematic phase. The phase separation and phase ordering process is characterized by simulating quenches into unstable and metastable regions of the phase diagram. Emerging two-dimensional morphologies include nematic emulsions and filled nematics. Droplets in nematic emulsions display the classical bipolar director field. The director field in filled nematics displays a stable defect polygonal network. Correlations between defect density and bi-phasic geometry are established and characterized using topological rules for liquid crystal defects.

1. Introduction

Design of multifunctional materials through blending of monomeric and polymeric precursors is a new avenue for new architectures. Polymer dispersed liquid crystals (PDLC) are industrially important materials which have attracted recent attention due to their mechanical and electro-optical properties. These bi-phasic optical materials are produced by phase separation processes and a rich variety of morphologies have been observed [1-2]. A great deal of attention has been directed to characterize the resulting morphologies, such as the typical bi-continuous and droplet morphologies. Phase separation of such systems can be induced either through a thermal quench [3-5] or through polymerization [6]. Due to a number of non-equilibrium processes involved, there is a little theoretical understanding of the factors that control the domain morphology. A Cahn-Hilliard framework that allows composition and orientational density to evolve in a coupled fashion as functions of position and time following a temperature quench was performed [4]. Their framework includes the tensorial nature of nematic order [7] but details of morphological structures, and characterization of morphological structures, phase separation and phase transition mechanism, topological defect structures remain poorly understood.

In this paper we present a dynamical model focusing on the interplay between phase-separation and phase ordering kinetics in mixtures of low molar mass liquid crystals (rigid rods) and long, flexible polymers, as a first step towards the rational design and control of the microdomain morphology. Here we consider fully nonlocal model without resorting to the three term gradient expansions of Landau-type [7] when derived free energy of the system. Computationally, this is challenging because it would require evaluating multiple convolutions at each moment in time. The advantage of our system is that we can calculate two order parameters (conserved and non-conserved) solving two coupled time-dependent equations together from a microscopic model of polymers and liquid crystals without loosing any information of order parameters.

2. Model Governing Equations

The dimensionless total free energy of the system consists of the bulk free energy and a nonlocal free energy that controls the cost of gradients in composition and orientational density, in the absence of surface terms and external fields, can be expressed as [8]

$$\tilde{F} = \tilde{T} \times \oint_{\tilde{v}} \left(\tilde{f}^h + \frac{1}{\tilde{T}} \tilde{f}^g \right) d\tilde{v}\,, \tag{1}$$

$$\tilde{f}^h = \left[\frac{\tilde{\varphi}}{n_I} \ln \tilde{\varphi} + \frac{(1-\tilde{\varphi})}{n_A} \ln(1-\tilde{\varphi}) + \chi \tilde{\varphi}(1-\tilde{\varphi}) + \frac{3}{4}\left(\frac{\tilde{\Gamma}_0}{n_A} \right)(1-\tilde{\varphi})^2 \tilde{Q} : \tilde{Q} - \frac{(1-\tilde{\varphi})}{n_A} \ln\left(\frac{\tilde{I}_0}{2} \right) \right], \tag{2}$$

$$\tilde{f}^{g}=\left[\frac{1}{2\tilde{D}}\times\left(\tilde{\nabla}\tilde{\varphi}\right)^{2}+\frac{\tilde{R}}{\tilde{D}}\times\left(\tilde{\partial}_{i}\tilde{\varphi}\right)\left(\tilde{\partial}_{j}\tilde{Q}_{ij}\right)\right.$$
$$\left.+\frac{\tilde{G}}{2\tilde{D}}\times\left(\tilde{\partial}_{k}\tilde{Q}_{ij}\right)^{2}+\frac{\tilde{P}}{2\tilde{D}}\times\left(\tilde{\partial}_{i}\tilde{Q}_{ik}\right)\left(\tilde{\partial}_{j}\tilde{Q}_{jk}\right)\right], \quad (3)$$

where

$$\tilde{I}_{0}=\int_{0}^{2\pi}\int_{0}^{\pi}exp\left[\frac{3}{2}\tilde{\Gamma}_{0}\left(1-\tilde{\varphi}\right)\tilde{\mathbf{Q}}:\left(\boldsymbol{\sigma\sigma}-\frac{\boldsymbol{\delta}}{3}\right)\right.$$
$$\left.sin^{2}\theta d\theta d\omega\right], \quad (4)$$

$$\tilde{\varphi}=\tilde{\varphi}_{\mathrm{I}},\ \tilde{\varphi}_{\mathrm{A}}=1-\tilde{\varphi},\ \tilde{\Gamma}_{0}=\left(\chi_{\mathrm{a}}+5/4\right)\mathrm{n}_{\mathrm{A}}. \quad (5)$$

where $\tilde{T}$ is the absolute temperature, χ is the Flory-Huggin's interaction parameter, $\boldsymbol{\sigma}$ is a unit vector and $\boldsymbol{\delta}$ denotes unit tensor, the terms χ_{a} and $(5/4)\mathrm{n}_{\mathrm{A}}$ in $\tilde{\Gamma}_{0}$ indicates the orientation-dependent attractive interactions between the mesogens and excluded volume interactions between mesogenic molecules respectively, n_{I} and n_{A} are the number of segments on the isotropic (monomer or polymer) component and the number of segments (axial ratios) on the mesogen respectively, and $\tilde{\varphi}_{\mathrm{I}}$ and $\tilde{\varphi}_{\mathrm{A}}$ are the corresponding volume fractions, respectively. $\tilde{\boldsymbol{Q}}$ is a second rank symmetric and traceless tensor [7,9] representing uniaxial state of liquid crystalline order, *S*, and average molecular orientation by **n**. $\tilde{D}$ is the dimensionless diffusion parameter, $\tilde{R}$ is the coupling parameter, $\tilde{G}$ and $\tilde{P}$ represent dimensionless Frank elastic parameters respectively. We defined the temperature parameter, τ, by $1/\tau=\chi=\mathrm{U}_{0}/\mathrm{k}_{\mathrm{b}}\mathrm{T}$, where U_{0} controls the miscibility of the two species in the isotropic phase and k_{b} is the Boltzmann constant.

As shown by De Gennes and Prost [7], equations (1-5) predict the emergence of a stable nematic phase when $\Gamma_{0}\varphi_{A}=4.55$. If we define:

$$\alpha=\chi_{\mathrm{a}}/\chi \quad (6)$$

where α represents the relative strength of interactions, it is found that the threshold $\tilde{\Gamma}_{0}\tilde{\varphi}_{A}=4.55$ gives the following concentration dependence of the reduced nematic-isotropic transition (NIT) temperature:

$$\tau_{\mathrm{NI}}\left(\tilde{\varphi}_{A}\right)=\frac{\alpha\,\mathrm{n}_{A}\tilde{\varphi}_{A}}{4.55-1.25\,\mathrm{n}_{A}\tilde{\varphi}_{A}}. \quad (7)$$

For simplicity, we denote the isotropic component composition by ϕ $\left(\phi\equiv\tilde{\varphi}\right)$ in the phase diagram (Fig 1).

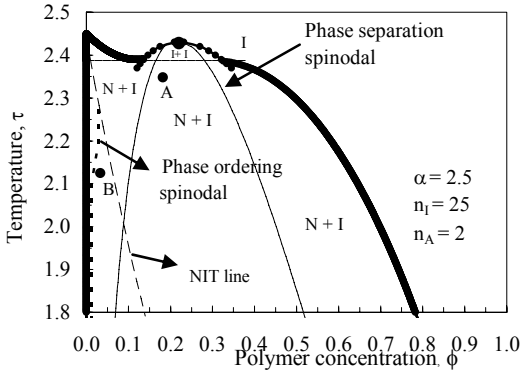

Fig. 1 Phase diagram of the binary mixtures of polymer and liquid crystals on the temperature–concentration plane for $n_{I}=25$, $n_{A}=2$, $\alpha=2.5$.

The dimensionless governing equations of the system then becomes [8]

$$\frac{\partial\tilde{\varphi}}{\partial\tilde{t}}=\left[\tilde{D}\times\tilde{T}\times\tilde{\nabla}^{2}\left(\frac{\partial\tilde{f}^{h}}{\partial\tilde{\varphi}}\right)-\tilde{\nabla}^{4}\tilde{\varphi}-\tilde{R}\times\tilde{\nabla}^{2}\left(\tilde{\nabla}\cdot\tilde{\nabla}\tilde{\mathbf{Q}}\right)\right], \quad (8)$$

$$\left[\frac{\partial\tilde{\mathbf{Q}}}{\partial\tilde{t}}\right]^{[s]}=\left[-\tilde{T}\times\tilde{D}\times\tilde{E}\times\frac{\partial\tilde{f}^{h}}{\partial\tilde{\mathbf{Q}}}+\tilde{E}\times\tilde{R}\times\tilde{\nabla}\cdot\tilde{\nabla}\tilde{\varphi}\right.$$
$$\left.+\tilde{E}\times\tilde{G}\times\tilde{\nabla}^{2}\tilde{\mathbf{Q}}+\tilde{E}\times\tilde{P}\times\tilde{\nabla}\left(\tilde{\nabla}.\tilde{\mathbf{Q}}\right)\right]^{[s]} \quad (9)$$

where $\tilde{t}$ is the dimensionless time and $\tilde{E}$ is the phenomenological constant. Dimensionless Eqs. (8)-(9) are solved by a high performance numerical scheme with periodic boundary condition [8].

3. Results and Discussions

A typical phase diagram of the system on the temperature-concentration plane is shown in Fig. 1. In the figure, ϕ, denotes the isotropic component composition (polymer concentration). The coexistence (binodal) curve of the phase equilibrium is derived by a double tangent method. Details procedure for construction of phase diagram for such a system is documented in the work [10]. Here we study the morphology following two temperature quenches from the isotropic, homogeneous phase into the isotropic-nematic (IN) coexistence region below the triple point line. Two regions are indicated by filled circles and denoted by points A and B respectively in the phase diagram (Fig. 1).

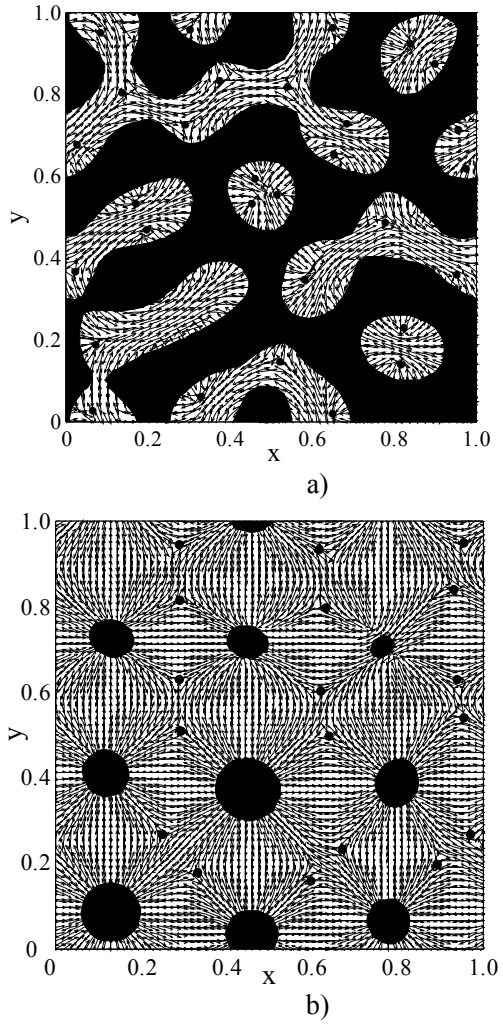

Fig. 2 Snapshot of the local composition of the system at a late time step following a quench to; a) point A and b) point B for $n_I = 25$, $n_A = 2$, $\alpha = 2.5$, $\tilde{D} = 1000$, $\tilde{E} = 1.0$, $\tilde{R} = 0.2$, $\tilde{G} = 0.1$, and $\tilde{P} = 0.1$. Black corresponds to isotropic polymer and white corresponds to pure liquid crystals (LCs). The arrows represent the local nematic director, and defects are marked with small solid circles.

Initially point A lying below the phase separation spinodal curve and above the NIT line corresponds to a state that is initially unstable with respect to phase separation but metastable with respect to phase ordering. At point B, between the NIT line and the nematic spinodal curve, the system is initially metastable with respect to phase separation but unstable with respect to the phase ordering. Fig. 2 represents the snapshot of compositional order of the system at points A and B respectively. In Fig. 2(a), mass matrix phase is isotropic and droplet phase is nematic. In Fig. 2(a) we can see that a pair of topological defects forms inside each microdomain due to the presence of repulsive Peach-Koehler forces. In our system the repulsive force naturally arises from interaction via the elastic deformation of liquid crystal [1,2].

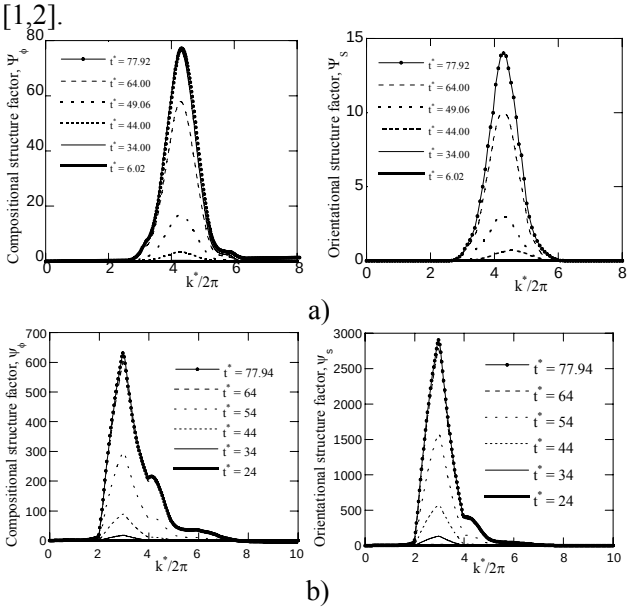

Fig. 3 Temporal evolution of compositional and orientational structure factors following a quench to; a) point A and b) point B for $n_I = 25$, $n_A = 2$, $\alpha = 2.5$, $\tilde{D} = 1000$, $\tilde{E} = 1.0$, $\tilde{R} = 0.2$, $\tilde{G} = 0.1$, and $\tilde{P} = 0.1$.

We can see from the Fig. 2(a) that orientation inside the droplet is perpendicular implying strong normal anchoring of liquid crystal molecules at the droplet boundary. Nematic droplets must develop defects because the LCs wants to be parallel to each other and parallel to the droplet interface too. This result agrees quite well with the results reported by Lapena *et.al* [4] (see Fig. 3, [4]). In Fig. 2(a), emerging textures show bi-continuous morphology. In Fig. 2(b), isotropic microdomains suspended into the nematic matrix are surrounded by the topological defects. One interesting feature of the defect lattice is its topology. Solid circles represent the defect cores. Defect structures form cellular polygonal networks that are mostly four-sided and the side of each polygon ends either at the droplet or at another defect. Most of the defects are +1/2 disclinations. Some of them are +1 disclinations eventually split into two +1/2 disclinations as can be seen from Fig. 2(b). In the case of point B (see Fig. 2(b)), microdomians are almost positionally ordered.

To get better understanding of underlying physics in phase separation and texture formation processes, we calculated the compositional and orientational structure factors at each of the quenching positions of

the system. Fig. 3 represents the temporal evolution of the compositional and orientational structure factors following quenches to the point A and B. In Fig. 3(a), we can clearly see that both compositional and orientational structure factors are almost similar in shape but magnitude at each of the time steps is different. It indicates that the maximum signal at each of the time step of compositional structure factors are much larger than the corresponding maximum signal of orientational structure factors for the case of nematic emulsion. It means that the compositional spinodal decomposition initially dominant in the phase separation and texture formation processes and accelerated nematic phase ordering by orientational spinodal decomposition. In Fig. 3(b), both the structure factors are similar in shape indicating that phase separation and phase ordering spinodal decomposition (SD) drives the system to be unstable, leading to the breakdown of the interconnected domains and formation of isotropic microdomains (droplets). The amplitude of orientational structure factors is larger than the compositional structure factors. This implies that the orientational spinodal decomposition is dominant in this quench and plays an important role for the breakdown of interconnected structure to form microdomain droplets morphology.

4. Conclusion

A tensor theory-based dynamic model for phase separation-phase ordering-texture formation has been formulated, and solved using high performance numerical methods. Emerging morphologies are characterized following two temperature quenches into the physically meaningful regions of phase diagram. It has been found that ordering dramatically affects morphology. Topological defects arise due to the elastic distortions around the microdomains formed during the phase separation. Defect structures form cellular polygonal networks that are mostly four-sided and the side of each polygon ends either at the droplet or at another defect. Both compositional and orientational structure factors of the system establish the dynamics and correlations of the morphological structures. Formation of interconnected (bicontinuous) networks or microdomins depends on whether ordering or phase separation is the initially dominant process. Compared to the experimental and numerical results available in the literature, our simulation results may able to provide new insights into the understanding of emerging microdomain topological defect morphology in liquid crystalline materials.

References

[1] National Research Council Report, Liquid Crystalline Polymers (National Academy Press, Washington, DC, 1990).

[2] J.W. Doane, Liquid Crystals: Applications and Uses, ed. B. Bahadur, World Scientific, NJ, 1990.

[3] P.S. Drzaic, Liquid crystal dispersions, World Scientific, Singapore, 1995.

[4] A.M. Lapena, S. C. Glotzer, S. A. Langer, and A.J. Liu, Phys. Rev. E 60(1), R29, 1999.

[5] M. Graca, S. A. Wieczorek, and R. Holyst, Macromolecules, 36, 6903-691, 2003.

[6] G.P. Crawford and S. Zumer, Liquid Crystals in Complex Geometries Formed by Polymer and Porous Networks, Taylor & Francis, London, 1996.

[7] P. G. de Gennes and J. Prost, The Physics of Liquid Crystals, Oxford University Press, NY, 1993.

[8] S. K. Das and A. D. Rey, Texture formation under phase ordering and phase separation in polymer and liquid crystal mixtures, J. Chem. Phys., **121**, 000, 2004, (to be appear).

[9] A.D. Rey and T. Tsuji, Macromol. Theory Simul. **7**, 623-639, 1998.

[10] S. K. Das and A. D. Rey, Computational Modelling of Multi-Phase Equilibria of Mesogenic Mixtures. J. Comp. Mat. Sci., **29(2)**, 152-164, 2004.